A powder tabletability equation

Gerrit Vreeman and Changquan Calvin Sun*

Pharmaceutical Materials Science and Engineering Laboratory, Department of Pharmaceutics, College of Pharmacy, University of Minnesota, Minneapolis, MN 55455, United States

**Corresponding author*

Changquan Calvin Sun, Ph. D.

9-127B Weaver-Densford Hall

308 Harvard Street S.E.

Minneapolis, MN 55455

Email: sunx0053@umn.edu

Tel: (612) 624-3722

Fax: (612) 626-2125

Abstract

An equation describing tablet tensile strength as a function of compaction pressure was derived from the Ryshkewitch and Kuentz-Leuenberger equations. The equation was used to fit data from 11 powders, including single-component powders and mixtures, with a wide range of mechanical properties. Three fitted parameters are obtained directly from tensile strength-compaction pressure data, of which one describes the apparent bonding strength and another strongly correlates with the plasticity.

Keywords: Tabletability, tableting, mechanical properties, tensile strength

1 Introduction

Compression properties of a powder can be systematically characterized by compressibility, tabletability, and compactibility (CTC) profiles, which capture the pairwise relationships among compaction pressure (P), tablet porosity (ε), and tablet tensile strength (σ) (Joiris et al., 1998; Tye et al., 2005). In the CTC approach, compressibility, tabletability, and compactibility refer to the ε–P, σ–P, and σ–ε relationships, respectively.

Among these relationships, tabletability is the most relevant to the manufacturability of a formulation because it predicts the pressure required to attain tablets with sufficient strength for surviving various stresses due to handling, shipping, and storage during the lifetime of a tablet. In this regard, σ is a tablet property critical to the success of a tablet product. Since σ is a result of the interplay between bonding area (BA) and bonding strength (BS) (Osei-Yeboah et al., 2016; Sun, 2011), mechanistic understanding of the tabletability of a given powder requires deconvolution of the contributions to σ from BA and BS. This can be partially achieved by considering porosity during the course of compression since the evolution of BA is accompanied by diminishing porosity.

Fitting compactibility data (σ–ε) with the Ryshkewitch equation (Equation 1) (Ryshkewitch, 1953), which describes this relationship as a negative exponential function, gives the tablet tensile strength at zero porosity (σ_0) and an empirical decay constant b.

$$\sigma = \sigma_0 e^{-b\varepsilon} \tag{1}$$

The σ_0 can quantify the apparent BS of a formulation, where a larger σ_0 exhibits a stronger apparent bonding strength. Here, the term “apparent BS” is used to recognize that σ_0 is not an intrinsic property of materials because it can vary with particle size and shape (Paul et al., 2019; Sun, 2011; Sun and Grant, 2004).

Compressibility data (ε–P), on the other hand, is used to characterize BA since a lower tablet porosity indicates a larger interparticulate BA for a given powder. Additionally, a material that can form a tablet with a lower porosity under a given compaction pressure is considered more plastic. Among several equations proposed for describing powder compressibility (Heckel, 1961a, 1961b; Kawakita and Lüdde, 1971; Kuentz and Leuenberger, 1999; Walker, 1923), the Kuentz and Leuenberger (KL) equation (Equation 2) best describes compressibility data over a wide range of pressures for most powders (Kuentz and Leuenberger, 1999; Sun, 2004).

$$P = \frac{1}{C}\left[(\varepsilon - \varepsilon_c) - \varepsilon_c \ln\left(\frac{\varepsilon}{\varepsilon_c}\right)\right] \quad (2)$$

In the KL equation, ε_c is critical porosity, and $1/C$ is a parameter in units of pressure that has been suggested to quantify powder plasticity (Paul and Sun, 2017a).

In contrast to the many equations proposed to describe both compactibility and compressibility, there is not yet an equation that can satisfactorily describe tabletability (σ–P). Persson and Alderborn approximated a tabletability profile using three discontinuous linear regions described by a lower critical pressure at which a coherent tablet can form (P_{c1}), an upper critical pressure at which the tensile strength plateau is reached (P_{c2}), and the pressure range between P_{c1} and P_{c2} at which tensile strength increases linearly according to effective particle hardness (Γ) (Persson and Alderborn, 2018). Others use empirically determined linear relationships to describe tabletability (Yu et al., 2020). However, both approaches do not completely describe tabletability profiles, which are non-linear. Leuenberger proposed an equation that describes the dependence of σ on both P and (1-ε), with some success (Leuenberger, 1982). However, the requirement of ε in this equation makes it practically less useful, as accurate determination of tablet porosity may not always be possible (Chang et al., 2019). However, the reliable mathematical expressions of the ε–P (the KL equation) and σ–ε (the Ryshkewitch equation) imply that a similarly reliable quantitative relationship between σ and P may exist. Hence, we set out to derive a tabletability equation and evaluate its performance using materials exhibiting a broad range of mechanical properties.

2 Theory

2.1 Derivation of the tabletability equation

Beginning with the KL equation (Equation 2), ε is solved in terms of P. The KL equation can be simplified into Equation 3.

$$PC + \varepsilon_c = \varepsilon + \ln\left(\frac{\varepsilon}{\varepsilon_c}\right)^{-\varepsilon_c} \tag{3}$$

Taking the exponential of both sides yields

$$e^{PC+\varepsilon_c} = e^{\varepsilon+\ln\left(\frac{\varepsilon}{\varepsilon_c}\right)^{-\varepsilon_c}} \tag{4}$$

Equation 5 is obtained by taking the -ε_c root and multiplying both sides by -1.

$$-e^{-\frac{PC}{\varepsilon_c}-1} = \left(-\frac{\varepsilon}{\varepsilon_c}\right)e^{-\frac{\varepsilon}{\varepsilon_c}} \tag{5}$$

Classically, equations with the generic form of $x = ye^y$ can be solved for y via the function $y = W(x)$ if $x \geq -e^{-1}$. Here, W is the Lambert function. Since P, C, and ε_c are always positive, $-e^{-\frac{PC}{\varepsilon_c}-1} \geq -e^{-1}$ for all valid values of P. Letting $x = -e^{-\frac{PC}{\varepsilon_c}-1}$ and $y = -\frac{\varepsilon}{\varepsilon_c}$, Equation 5 can be expressed as Equation 6.

$$-\frac{\varepsilon}{\varepsilon_c} = W\left(-e^{-\frac{PC}{\varepsilon_c}-1}\right) \tag{6}$$

Rearranging to isolate ε Equation 7 becomes

$$\varepsilon = -\varepsilon_c W\left(-e^{-\frac{PC}{\varepsilon_c}-1}\right) \tag{7}$$

Equation 7 describes compressibility (ε versus P) equivalently to the KL equation. Combining Equation 7 with the Ryshkewitch equation (Equation 1) yields Equation 8, which describes σ as a function of P.

$$\sigma = \sigma_0 e^{b\varepsilon_c W\left(-e^{-\frac{PC}{\varepsilon_c}-1}\right)} \tag{8}$$

Here, σ_0 and b are the constants in the Ryshkewitch equation (Equation 1), and ε_c and C are constants in the KL equation (Equation 2). To avoid multi-collinearity during nonlinear regression of tabletability data using this equation, we define $b\varepsilon_c=\alpha$ and $\varepsilon_c/C = \beta$. Thus, α is b from the Ryshkewitch equation scaled by ε_c, and β is $1/C$ from the KL equation scaled by ε_c. Additionally, σ_0 is redefined as σ_{max} since this parameter is obtained from nonlinear regression between σ and P without considering porosity. Following these substitutions, Equation 8 can be simplified to Equation 9, which can be used to fit σ–P data directly.

$$\sigma = \sigma_{max} e^{\alpha W\left(-e^{-\frac{P}{\beta}-1}\right)} \tag{9}$$

It may be noted that since $-e^{-1} \leq -e^{-\frac{P}{\beta}-1} \leq 0$, there are always two solutions to $W\left(-e^{-\frac{P}{\beta}-1}\right)$ that exist on the principal (W_0) branch and the W_{-1} branch, respectively (Corless et al., 1996). However, only solutions to the principal branch can sensibly describe tabletability data because σ is expected to increase with applied pressure. Moreover, it is noted that $\lim_{P\to 0} W_0\left(-e^{-\frac{P}{\beta}-1}\right) = -1$, which results in $\sigma = \sigma_{max}e^{-\alpha}$, and that $\lim_{P\to\infty} W_0\left(-e^{-\frac{P}{\beta}-1}\right) = 0$, which results in $\sigma = \sigma_{max}$. The Lambert W function is available in many common statistical software packages that may be used for nonlinear regression.

2.2 Impact of parameters on the shape of tabletability profile

Equation 9 describes an asymmetric sigmoidal function (Figure 1). The parameter σ_{max} describes the tensile strength as compaction pressure approaches infinity (Figure 1a). Thus, different σ_{max} values alter the asymptotic plateau at sufficiently high pressures. The parameter α describes the width of the convex portion of the tabletability curve in the low-pressure region (Figure 1b) and may correlate with packing efficiency and change with particle size or shape. Finally, the parameter β describes the curvature of the concave region, i.e., the onset of the plateau in σ with respect to P (Figure 1c).

Highly plastic materials are typically described as having tabletability profiles that exhibit a swift rise in tensile strength followed by a plateau as the density of more plastic materials will more quickly approach their true density with an increase in compaction pressure (Sun, 2005; Sun et al., 2018). Based on this observation and the influence of β on the shape of the tabletability profile (Figure 1c), β may be related to the plasticity of the powder. This is aligned with the fact that β is essentially $1/C$, which has been established as a highly reliable measure of material plasticity (Paul and Sun, 2017a), scaled by ε_c and is in units of pressure. A distinct advantage of the parameter β is that it can be obtained from tabletability profiles using Equation 9 without considering ε, which may not be accurately determined for materials containing volatile components (Chang et al., 2019; Sun, 2006).

2.3 An alternative tabletability equation

Equation 9 is similar to the Gompertz function (Gompertz, 1825), which is a double exponential function that describes an asymmetric sigmoidal curve (Equation 10) and has been extensively used to model biological growth (Aggrey, 2002; Benzekry et al., 2014; Tjørve and Tjørve, 2017; Winsor, 1932).

$$y = y_{max} e^{-e^{-k(x-x_0)}} \tag{10}$$

In Equation 10, y_{max} is the asymptotic value as x approaches infinity, k is a growth constant, and x_0 is the inflection point at the center of the curve where the convex curve becomes concave. However, a detailed comparison of Equation 9 to the Gompertz function (see supplemental information) shows that Equation 9 is superior to the Gompertz function for realistically describing tabletability data in the low-pressure region.

3 Methods and Materials

3.1 Materials

Microcrystalline cellulose (MCC; Avicel PH102, FMC Biopolymer, Philadelphia, PA), dicalcium phosphate dihydrate (DCPD; Emcompress®, JRS Pharma, Patterson, NY), dicalcium phosphate anhydrous (DCPA; Emcompress®, JRS Pharma, Patterson, NY), lactose monohydrate (LM; #316 Fastflo® NF, Foremost Farms, Clayton, WI), mannitol 200SD (Mann; Pearlitol® 200SD, Roquette America Inc., Keokuk, IA), urea (Fisher Scientific, Hampton, NH), and ferulic acid (FA; Sigma Aldrich, St. Louis, MO) were used as received.

The binary mixtures of 90%, 75%, and 50% (w/w) DCPA with MCC were prepared by mixing in a blender (Turbula, Glen Mills, Clifton, NJ) at 49 rpm for 5 min. A mixture of MCC with 1% (w/w) magnesium stearate (MgSt; non-bovine, HyQual™, Mallinckrodt, St. Louis, MO) was also prepared by blending at 49 rpm for 2 min.

3.2 Tablet compression

Tablets were made using a compaction simulator (Styl'One, MedelPharm, Beynost, France) using a 2% single compression cycle, composed of a 2 s compression (1 s rise and 1 s fall with no holding time at the maximum force) followed by a 3 s relaxation and a 2 s ejection step. Magnesium stearate spray (Styl'One MIST) was used to externally lubricate the die wall and punch tips before each compression for all materials except MCC and MCC+1% MgSt.

3.3 Tablet tensile strength

Tablet tensile strength was determined by measuring tablet dimensions using a digital caliper (model CD-6"AX, Mitutoyo, Kawasaki, Kanagawa, Japan) and tablet breaking force using a texture analyzer (TA-XT2i; Texture Technologies Corporation, Scarsdale, NY). Tablet tensile strength (σ) was calculated using Equation 11 following a standard procedure (Fell and Newton, 1970).

$$\sigma = \frac{2F}{\pi D t} \tag{11}$$

Where F is the tablet breaking force, D is the measured tablet diameter, and t is tablet thickness.

3.4 Tablet porosity

The true density (ρ_t) was determined using helium pycnometry (Quantachrome Instruments, Ultrapycnometer 1000e, Boynton Beach, Florida) with an accurately weighed sample (~1.5 g) filling about 75% of the volume of the sample cell. An analytical balance (Mettler Toledo, Columbus, Ohio, model AG204) was used to determine the mass. The experiment was stopped when the coefficient of variation between five consecutive measurements was below 0.005%, and the mean of the last five measurements was taken as the measured true density. Tablet porosity (ε) was calculated according to Equation 12.

$$\varepsilon = 1 - \frac{\rho}{\rho_t} \tag{12}$$

Where ρ is tablet density.

3.5 In-die Heckel analysis

In-die ε data was calculated from tablet thickness measured with the compaction simulator and the weight of the ejected tablet. Mean yield pressure (P_y) was obtained from a linear regression of the linear portion of the Heckel plot (-ln(ε) versus P) according to Equation 13 (Heckel, 1961a, 1961b).

$$-\ln(\varepsilon) = \frac{1}{P_y}P + A \tag{13}$$

3.6 Nonlinear regression and data fitting

Nonlinear regression of tabletability data to Equation 9 was performed in Python (v3.9.11) using SciPy's (v1.8.0) orthogonal distance regression library using ordinary least-squares optimization (job=2). The Lambert W function was implemented using SciPy's special functions library, and principal branch solutions were selected by default. Bootstrapped confidence intervals were obtained by resampling and curve-fitting the data 1000 times.

4 Results and Discussion

4.1 Validating the tabletability equation

The tabletability profiles of MCC, MCC with 1% MgSt, FA, Mann, urea, LM, and DCPD (Figure 2a), and DCPA blends with MCC (Figure 2b) can all be well described by Equation 9.

Table S1 contains the fitted parameters for all 11 powders according to Equation 9. The α values for the 11 powders fall in the range of 4 to 7 with low relative error. Accurate determination of β is entirely dependent on access to the concave curvature of the tabletability curve. For example, the concave portion of the tabletability curve of DCPA and DCPD cannot be experimentally accessed. For DCPA, lamination occurred at 500 MPa (Figure 2b). The lack of data in the concave portion of the tabletability curve leads to the large relative standard errors of both σ_{max} and β (Table S1). This is why a wide confidence interval of σ for DCPD was observed when extrapolated to high pressures (Figure 3a).

To further probe the implication of the absence of data in the concave region of the tabletability profile, data points from the concave region of the tabletability curve of MCC and urea were excluded, and fitting was repeated (Figure 3b). For both MCC and urea, the absence of the concave curvature results in an underestimated σ_{max} and β and a slightly overestimated α compared to the parameters fitted with the entire profiles. The excluded data points lie above the fitted line but within the 95% confidence interval. Thus, it is likely that the σ_{max} and β values for DCPD and mixtures of DCPA with MCC (Table S1) are also underestimated since the concave portion of the curves is not directly apparent (Figure 2).

Although the physical meaning of α has yet to be determined, a larger α corresponds to a tabletability profile with a delayed onset of developing considerable σ (Figure 1b), i.e., higher pressure is required to form a structure exhibiting appreciable mechanical rigidity. The physical meaning of β is more apparent since it generally correlates with in-die P_y (Table S1), with more plastic materials exhibiting lower β values. The ability of β to predict material plasticity, which affects the bonding area, would be useful. This is particularly valuable as it would provide a method of plasticity determination independent from material porosity, thus circumventing tablet density and true density measurements.

If β is a predictor of material plasticity, a strong correlation with other plasticity parameters is expected. However, a comparison of β values of the 11 powders to their in-die P_y values, obtained from an in-die Heckel analysis (Figure S1), shows high variability and a relatively low R^2 when fitted with the power-law function (Figure 4, red line). This poor correlation is likely caused by the underestimated β for the harder, high β materials, as previously discussed. Accurate β values should result in a stronger correlation with the in-die P_y. To verify this, σ_{max} was fixed at σ_0, obtained by fitting compactibility data using the Ryshkewitch equation (Figure S2), and α and β were redetermined using nonlinear regression (Figure S3, Table S1). The fitted β values are significantly higher and correlate strongly with P_y, following a power-law relationship (Figure 4, blue line). Thus, for very hard materials, the Ryshkewitch equation may be used to determine an accurate σ_{max} to aid accurate fitting to Equation 9, with the caveat that accurate porosity measurements must be employed. β obtained with and without fixing σ_{max} at σ_0 is very similar for low β powders (Figure S4). Thus, for more plastic powders, an accurate β may be obtained directly from tabletability plots as long as the concave region of the curve is apparent.

This analysis indicates that, when accurately measured, β is highly correlated with in-die P_y. This is also supported by the strong correlation between β (i.e., $1/C$ scaled by ε_c) versus in-die P_y data obtained from the literature (Figure S5). Both the β of the tabletability equation in this work and the Γ in the Persson and Alderborn approach are related to plasticity of materials (Persson and Alderborn, 2018).

4.2 Potential applications of the tabletability equation

Equation 9 can accurately capture the tabletability of different materials using three constants; and hence, provide a way to concisely describe a material's tabletability. The fitted relationships can be compared and evaluated as a function of process parameters and formulation composition to guide formulation optimization and aid process scale-up. Additionally, this analysis does not require any special instrument other than those routinely used to make tablets at different pressures, measure tablet dimensions, and determine tablet breaking force.

Equation 9 predicts a continuous increase in tablet tensile strength with rising compaction pressure until a plateau is reached. Therefore, if a decrease in tensile strength is observed upon increasing compaction pressure due to overcompression (Paul and Sun, 2017b), such data points can be excluded before fitting with Equation 9. This is shown for FA, Mann, and DCPA in Figure 2, where open symbols signify overcompressed tablets.

Equation 9 is valid for any powder well described by both the Ryshkewitch (Equation 1) and KL equations (Equation 2). Practically, adequate data points spanning a pressure range covering the concave region of the tabletability curve are required. Consequently, this equation cannot be applied to drugs that do not form intact tablets by compression. However, since adequate tabletability is a prerequisite for tablet manufacturing, this approach can be applied to characterize the compaction behavior of most appropriately-designed tablet formulations. Problems that prevent the reliable application of this equation invariably signify inherent problems with their tabletability.

5 Conclusion

A new tabletability equation, derived from the porosity-based Ryshkewitch and KL equations, can accurately describe the relationship between tablet tensile strength and compaction pressure of 11 powders exhibiting a wide range of mechanical properties and compaction behaviors. It describes the entire tabletability profile using three constants, where two of them quantify the maximum tensile strength attainable by a powder and its plasticity. This provides a means for assessing plasticity without considering tablet porosity, which is particularly beneficial for powders with error-prone true densities that make it difficult to calculate accurate tablet porosities.

6 Acknowledgments

Funding from the National Science Foundation through grant number IIP- 1919037 is gratefully acknowledged for partially supporting G.V. CCS thanks the National Science Foundation for support through the Industry University Collaborative Research Center grant IIP-2137264, Center for Integrated Materials Science and Engineering for Pharmaceutical Products (CIMSEPP).

References

Aggrey, S., 2002. Comparison of three nonlinear and spline regression models for describing chicken growth curves. Poultry Science 81, 1782–1788. https://doi.org/10.1093/ps/81.12.1782

Benzekry, S., Lamont, C., Beheshti, A., Tracz, A., Ebos, J.M.L., Hlatky, L., Hahnfeldt, P., 2014. Classical mathematical models for description and prediction of experimental tumor growth. PLOS Computational Biology 10, e1003800. https://doi.org/10.1371/journal.pcbi.1003800

Chang, S.-Y., Wang, C., Sun, C.C., 2019. Relationship between hydrate stability and accuracy of true density measured by helium pycnometry. International Journal of Pharmaceutics 567, 118444. https://doi.org/10.1016/j.ijpharm.2019.06.035

Corless, R.M., Gonnet, G.H., Hare, D.E.G., Jeffrey, D.J., Knuth, D.E., 1996. On the Lambert W function. Advances in Computational Mathematics 5, 329–359. https://doi.org/10.1007/BF02124750

Fell, J.T., Newton, J.M., 1970. Determination of tablet strength by the diametral-compression test. Journal of Pharmaceutical Sciences 59, 688–691. https://doi.org/10.1002/jps.2600590523

Gompertz, B., 1825. XXIV. On the nature of the function expressive of the law of human mortality, and on a new mode of determining the value of life contingencies. In a letter to Francis Baily, Esq. F. R. S. &c. Philosophical Transactions of the Royal Society of London 115, 513–583. https://doi.org/10.1098/rstl.1825.0026

Heckel, R.W., 1961a. Density-pressure relationships in powder compaction. Trans. Metall. Soc. AIME 221, 671–675.

Heckel, R.W., 1961b. An analysis of powder compaction phenomena. Trans. Metall. Soc. AIME 221, 1001–1008.

Joiris, E., Martino, P.D., Berneron, C., Guyot-Hermann, A.-M., Guyot, J.-C., 1998. Compression behavior of orthorhombic paracetamol. Pharmaceutical Research 15, 1122–1130. https://doi.org/10.1023/A:1011954800246

Kawakita, K., Lüdde, K.-H., 1971. Some considerations on powder compression equations. Powder Technology 4, 61–68. https://doi.org/10.1016/0032-5910(71)80001-3

Kuentz, M., Leuenberger, H., 1999. Pressure susceptibility of polymer tablets as a critical property: A modified Heckel equation. Journal of Pharmaceutical Sciences 88, 174–179. https://doi.org/10.1021/js980369a

Leuenberger, H., 1982. The compressibility and compactibility of powder systems. International Journal of Pharmaceutics 12, 41–55. https://doi.org/10.1016/0378-5173(82)90132-6

Osei-Yeboah, F., Chang, S.-Y., Sun, C.C., 2016. A critical examination of the phenomenon of bonding area - bonding strength interplay in powder tableting. Pharmaceutical Research 33, 1126–1132. https://doi.org/10.1007/s11095-016-1858-8

Paul, S., Sun, C.C., 2017a. The suitability of common compressibility equations for characterizing plasticity of diverse powders. International Journal of Pharmaceutics 532, 124–130. https://doi.org/10.1016/j.ijpharm.2017.08.096

Paul, S., Sun, C.C., 2017b. Gaining insight into tablet capping tendency from compaction simulation. International Journal of Pharmaceutics 524, 111–120. https://doi.org/10.1016/j.ijpharm.2017.03.073

Paul, S., Tajarobi, P., Boissier, C., Sun, C.C., 2019. Tableting performance of various mannitol and lactose grades assessed by compaction simulation and chemometrical analysis. International Journal of Pharmaceutics 566, 24–31. https://doi.org/10.1016/j.ijpharm.2019.05.030

Persson, A.-S., Alderborn, G., 2018. A hybrid approach to predict the relationship between tablet tensile strength and compaction pressure using analytical powder compression. European Journal of Pharmaceutics and Biopharmaceutics 125, 28–37. https://doi.org/10.1016/j.ejpb.2017.12.011

Ryshkewitch, E., 1953. Compression strength of porous sintered alumina and zirconia. Journal of the American Ceramic Society 36, 65–68. https://doi.org/10.1111/j.1151-2916.1953.tb12837.x

Sun, C.C., 2011. Decoding powder tabletability: roles of particle adhesion and plasticity. Journal of Adhesion Science and Technology 25, 483–499. https://doi.org/10.1163/016942410X525678

Sun, C.C., 2006. A material-sparing method for simultaneous determination of true density and powder compaction properties—Aspartame as an example. International Journal of Pharmaceutics 326, 94–99. https://doi.org/10.1016/j.ijpharm.2006.07.016

Sun, C.C., 2005. True density of microcrystalline cellulose. Journal of Pharmaceutical Sciences 94, 2132–2134. https://doi.org/10.1002/jps.20459

Sun, C.C., 2004. A novel method for deriving true density of pharmaceutical solids including hydrates and water-containing powders. Journal of Pharmaceutical Sciences 93, 646–653. https://doi.org/10.1002/jps.10595

Sun, C.C., Grant, D.J.W., 2004. Improved tableting properties of p-hydroxybenzoic acid by water of crystallization: A molecular insight. Pharmaceutical Research 21, 382–386. https://doi.org/10.1023/B:PHAM.0000016272.81390.b4

Sun, W.-J., Kothari, S., Sun, C.C., 2018. The relationship among tensile strength, young's modulus, and indentation hardness of pharmaceutical compacts. Powder Technology 331, 1–6. https://doi.org/10.1016/j.powtec.2018.02.051

Tjørve, K.M.C., Tjørve, E., 2017. The use of Gompertz models in growth analyses, and new Gompertz-model approach: An addition to the Unified-Richards family. PLOS ONE 12, e0178691. https://doi.org/10.1371/journal.pone.0178691

Tye, C.K., Sun, C.C., Amidon, G.E., 2005. Evaluation of the effects of tableting speed on the relationships between compaction pressure, tablet tensile strength, and tablet solid fraction. Journal of Pharmaceutical Sciences 94, 465–472. https://doi.org/10.1002/jps.20262

Walker, E.E., 1923. The properties of powders. part VI. the compressibility of powders. Trans. Faraday Soc. 19, 73–82. https://doi.org/10.1039/TF9231900073

Winsor, C.P., 1932. The Gompertz curve as a growth curve. Proceedings of the National Academy of Sciences 18, 1–8. https://doi.org/10.1073/pnas.18.1.1

Yu, Y., Zhao, L., Lin, X., Wang, Y., Feng, Y., 2020. A model to simultaneously evaluate the compressibility and compactibility of a powder based on the compression ratio. International Journal of Pharmaceutics 577, 119023. https://doi.org/10.1016/j.ijpharm.2020.119023

Figure Legends

Figure 1. Theoretical tabletability profiles using different combinations of the three parameters in Equation 9. One parameter was systematically varied while keeping the other two unchanged to show the impact of each parameter on the shape of the profile, **(a)** σ_{max}, **(b)** α, **(c)** and β values.

Figure 2. Tensile strength versus compaction pressure fitted with Equation 9 for (**a**) various excipients and APIs and (**b**) physical mixtures of MCC with DCPA**.** Markers plotted with open symbols indicate overcompressed tablets, where tensile strength decreases as compaction pressure increases and are not included in the fitting. Error bars are present in both x and y directions but are sometimes hidden by the symbols.

Figure 3. (**a**) The DCPD tabletability curve fitted with Equation 9 and a bootstrapped 95% confidence intervals projected to high pressures, and (**b**) MCC and urea with points from the concave region of the curve excluded from fitting to mimic the tabletability curve observed in DCPD. Open symbols represent data omitted from fitting.

Figure 4: β versus P_y for materials listed in Table S1. The blue and red fitted line and data point represent fitting to Equation 9 with and without fixing σ_{max} at σ_0 obtained from the Ryshkewitch equation, respectively.

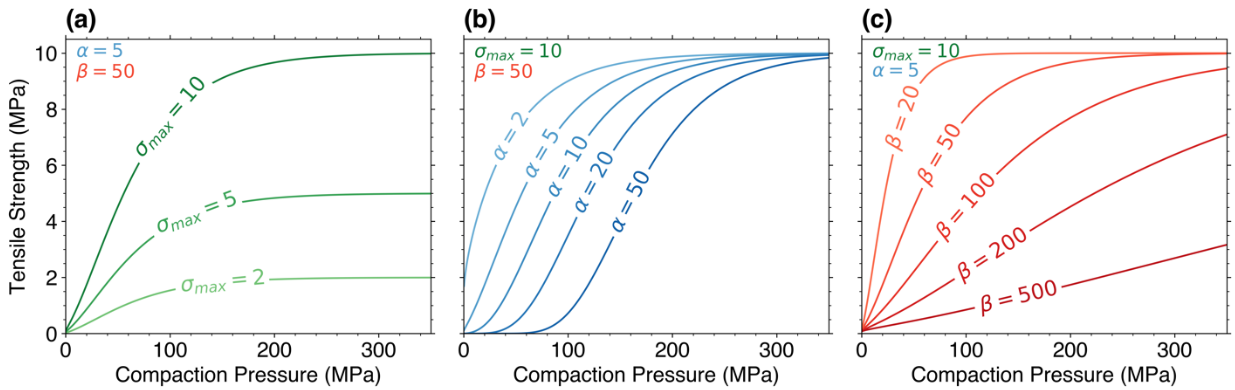

Figure 1. Theoretical tabletability profiles using different combinations of the three parameters in Equation 9. One parameter was systematically varied while keeping the other two unchanged to show the impact of each parameter on the shape of the profile, **(a)** σ_{max}, **(b)** α, **(c)** and β values.

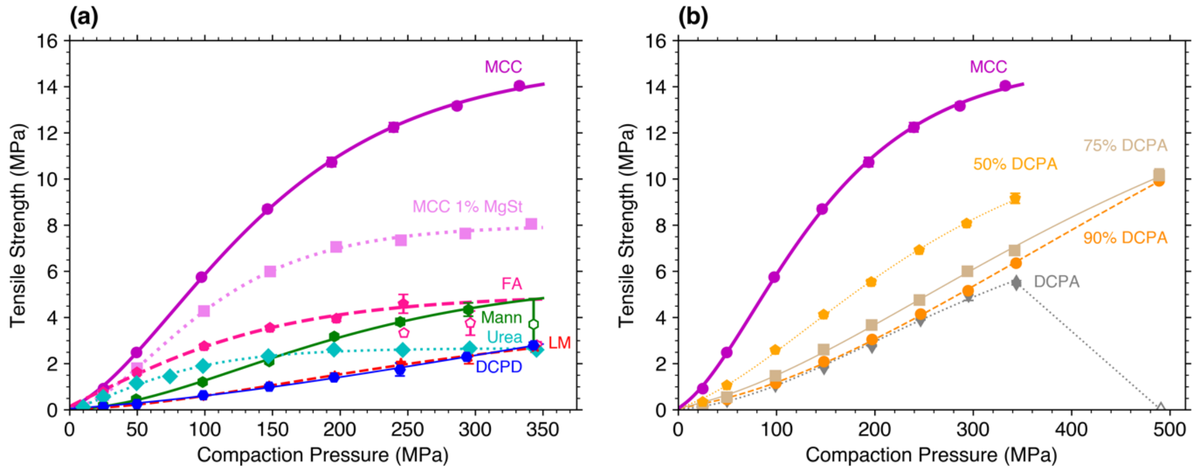

Figure 2. Tensile strength versus compaction pressure fitted with Equation 9 for (**a**) various excipients and APIs and (**b**) physical mixtures of MCC with DCPA**.** Markers plotted with open symbols indicate overcompressed tablets, where tensile strength decreases as compaction pressure increases and are not included in the fitting. Error bars are present in both *x* and *y* directions but are sometimes hidden by the symbols.

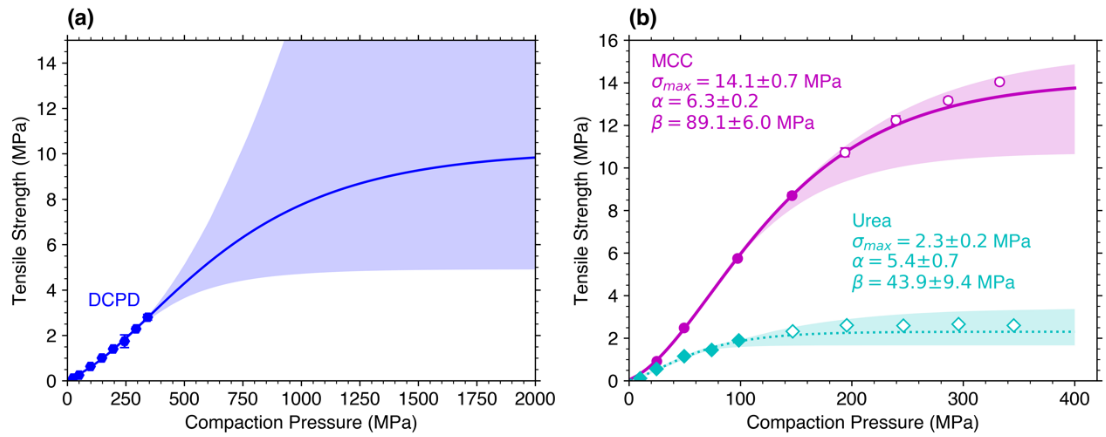

Figure 3. (**a**) The DCPD tabletability curve fitted with Equation 9 and a bootstrapped 95% confidence intervals projected to high pressures, and (**b**) MCC and urea with points from the concave region of the curve excluded from fitting to mimic the tabletability curve observed in DCPD. Open symbols represent data omitted from fitting.

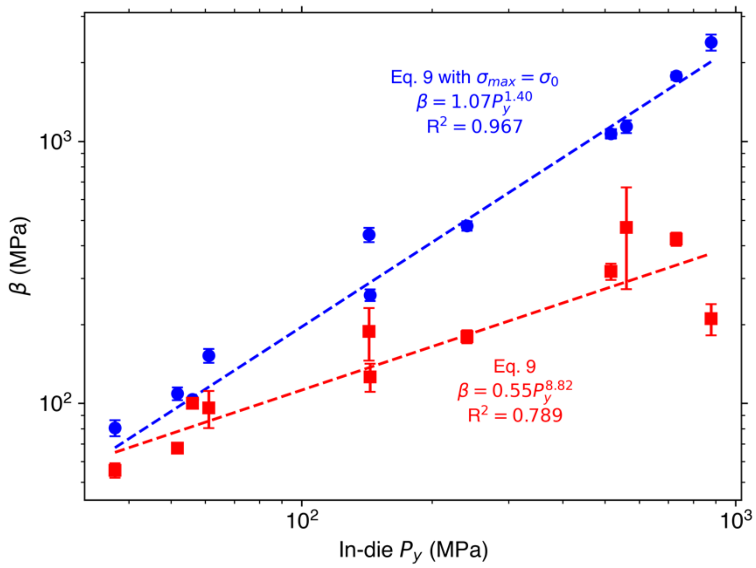

Figure 4: β versus P_y for materials listed in Table S1. The blue and red fitted line and data point represent fitting to Equation 9 with and without fixing σ_{max} at σ_0 obtained from the Ryshkewitch equation, respectively.

Credit Author Statement

Gerrit Vreeman: Methodology, Formal analysis, Investigation, Writing- Original draft preparation.

Changquan Calvin Sun: Supervision, Conceptualization, Writing- Reviewing and Editing, Resources, Funding acquisition

Declaration of interests

☒ The authors declare that they have no known competing financial interests or personal relationships that could have appeared to influence the work reported in this paper.

☐The authors declare the following financial interests/personal relationships which may be considered as potential competing interests:

Click here to access/download
Supplementary Material
(final, 3rd submission) SI.docx